Phase Contribution of Image Potential on Empty Quantum Well States in Pb Islands on the Cu(111) Surface

M. C. Yang,[1,2] C. L. Lin,[1] W. B. Su,[1] S. P. Lin,[1,3] S. M. Lu,[1,4] H. Y. Lin,[3] C. S. Chang,[1] W. K. Hsu,[2] and Tien T. Tsong[1]

[1]*Institute of Physics, Academia Sinica, Nankang, Taipei 115, Taiwan, ROC*

[2]*Department of Materials Science and Engineering, National Tsing Hua University, Hsinchu, Taiwan, Republic of China*

[3]*Department of Materials Science and Engineering, National Dong Hwa University, Hualien 974, Taiwan, Republic of China*

[4]*Department of Physics, Tunghai University, Taichung 407, Taiwan, Republic of China*

(Received 11 January 2009; published 12 May 2009)

We use scanning tunneling spectroscopy to explore the quantum well states in the Pb islands grown on a Cu(111) surface. Our observation demonstrates that the empty quantum well states, whose energy levels lie beyond 1.2 eV above the Fermi level, are significantly affected by the image potential. As the quantum number increases, the energy separation between adjacent states is shrinking rather than widening, contrary to the prediction for a square potential well. By simply introducing a phase factor to reckon the effect of the image potential, the shrinking behavior of the energy separation can be reasonably explained with the phase accumulation model. The model also reveals that there exists a quantum regime above the Pb surface in which the image potential is vanished. Moreover, the quasi-image-potential state in the tunneling gap is quenched because of the existence of the quantum well states.

DOI: 10.1103/PhysRevLett.102.196102 PACS numbers: 68.37.Ef, 68.65.Fg, 73.21.Fg

Electrons in metallic films with atomic-scale flatness and nanometer thickness can lead to the formation of quantum well (QW) states, which has been intensely studied by photoemission spectroscopy [1–5] as well as scanning tunneling microscopy and spectroscopy (STM and STS) [6–11]. Experimental studies have also demonstrated that the manifestation of the QW states can affect physical properties of the film, such as electrical resistivity [12], interlayer spacing [8,13], island coarsening [14], thermal stability [15], superconductivity temperature [16,17], Kondo temperature [18,19], thermal expansion coefficient [20], and so forth.

The solution of Schrödinger equation predicts that the energy level of a quantized state in the square potential well is proportional to n^2, where n is the quantum number. Therefore, the energy separation between adjacent quantized state should increase monotonically with increasing quantum number. In this Letter, we study the QW states in the Pb film grown on Cu(111) surface [9] with STM and STS. Our observation shows that the energy separations for the QW states around the Fermi level indeed increase with increasing the quantum number. However, for the empty QW states whose energy level lies above 1.2 eV from the Fermi level, the energy separation reveals a decreasing trend. This implies the potential form in the film near the vacuum level cannot be approximated by a simple square shape. In fact, the theoretical work did point out that the image potential would significantly modify the potential at the surface-vacuum interface, especially at the region close to the vacuum level [21]. It can thus be inferred that this unusual behavior of the QW states is associated with the existence of image potential. In this work, we introduce a phase contribution for the image potential in the phase accumulation model [22–24] to calculate the energies of the QW states. The calculated results indeed manifest the effect of the image potential and describe the phenomenon of shrinking energy separations among the higher lying QW states. Furthermore, our calculation also reveals that above the Pb surface, there exists a quantum regime where electrons are unable to feel the image potential. This is because the electrons can penetrate into the side of the square well.

Previous studies have demonstrated that Pb can be grown into flat islands with (111) orientation on Cu(111) surface at room temperature, and the electronic structures of islands involve the QW states [25]. In our experiment, we use a homebuilt STM operating at 4.3 K to observe the QW states. In contrast to the conventional I-V spectroscopy, here we use the Z-V spectroscopy, which enables the probing of higher energy QW states. Differentiation of a Z-V spectrum was performed by a numerical method.

Figure 1(a) shows a typical topographic image of the Pb film grown on Cu(111) surface with a coverage of 2.1 ML. Before the island's formation, about 1 ML Pb was consumed in wetting the Cu(111) substrate. The rest of Pb grew into islands above the wetting layer. Islands of different thickness can be observed because the growth did not follow the layer-by-layer mode. The thickness was measured against the exposed wetting layer. The QW states in Pb films on the Cu(111) surface were measured previously by Otero *et al.* [25] using I-V spectroscopy. One might argue that the QW states detected here using Z-V spectroscopy would not be identical to the ones obtained by I-V spectroscopy. In order to check their consistency, we performed the measurements on the film of 17-layer thickness with both kinds of spectroscopy, as shown in Fig. 1(b). It can be seen that the last two QW peaks of higher energy in the dZ/dV-V spectrum are identical to those in the

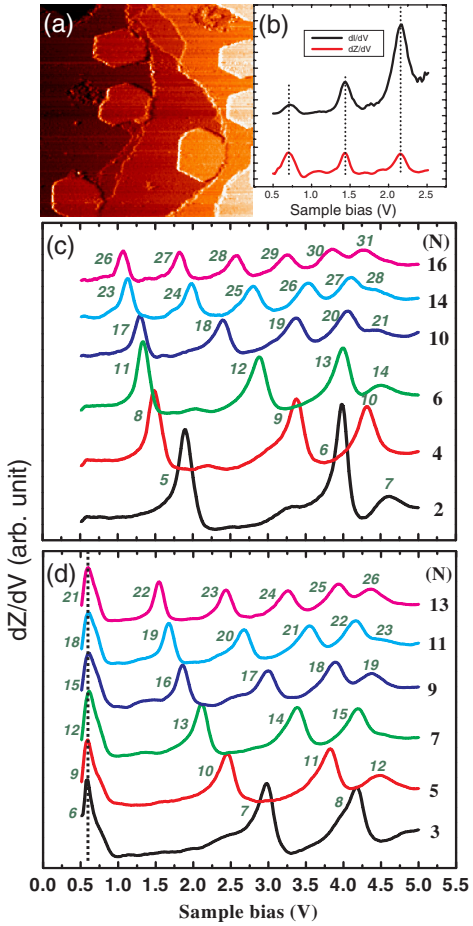

FIG. 1 (color online). (a) The growth of Pb islands on Cu(111) surface at room temperature at the coverage of 2.1 ML. The image size is 100×100 nm. (b) Comparison of differential spectra acquired from I-V and Z-V spectroscopy on the island of 17-layer thickness. Dashed lines mark the peaks in the dZ/dV-V spectrum. (c) and (d) are dZ/dV-V spectra acquired on the island of different thickness represented with the number of atomic layers. The spectra are grouped into the odd and the even number group in (c) and (d), respectively.

dI/dV-V spectrum, indicated with the dashed lines. However, there is an observable difference about 0.02 eV between the lowest peaks. This energy difference is likely due to the effect of electric field in the tunneling gap [26]. The strength of the electric field while taking the I-V and Z-V spectra may be substantially different, causing a minute shift in the position of the lowest peak. Based on the same reason, the positions of last two peaks may not coincide at the different condition.

Figures 1(c) and 1(d) display dZ/dV-V spectra acquired on Pb islands of different thickness in the energy range of 0.5–5 eV above the Fermi level. The number N at the right-hand side of each spectrum represents the island thickness in terms of atomic layers, and the spectra are grouped into the even and odd numbers in Figs. 1(c) and 1(d), respectively. Figure 1(c) lacks 8- and 12-layer spectra because islands with these two kinds of thickness are difficult to be found [9]. Peaks in each spectrum represent the QW states and the amount of peaks increases for a thicker island. While the positions of most of peaks change with the thickness, a peak located at 0.6 eV above the Fermi level [indicated by a dashed line in Fig. 1(d)] is clearly independent of the thickness. Previous studies have identified that the wave vector k of this specific QW state is $3\pi/2d$ [8], where d equal to 2.86 Å is the interlayer spacing of Pb island along the $\langle 111 \rangle$ direction. The existence of this peak implies that the finite square well in an island can be approximated by the infinite square well with a width of $W = Md$. The value of M must be an even integer and larger than N because electrons can penetrate into both sides of a finite square barrier. Since N in Fig. 1(d) is the odd number, M could be equal to $(N + 1)$, $(N + 3)$, $(N + 5)$, and so on. We can use the energy separation between first two peaks (from left end) in each spectrum in Figs. 1(c) and 1(d) to judge which relationship is valid. The quantization condition for the infinite potential well is $kMd = n\pi$, where n is a quantum number. Since the wave vector of the thickness-independent peak is known, we can assign each peak with a corresponding quantum number and calculate the energy separation ΔE between first two peaks using the equation

$$\Delta E = \hbar^2(2n + 1)\pi^2/2m^*W^2, \quad (1)$$

where n is the quantum number of low-energy peak and m^* is the effective mass in the [111] direction, which is $1.14m_0$ [12]. Figures 2(a) and 2(b) show that the energy separation as function of thickness for the experimental measurements and the calculation results of $M = (N + 1)$, $(N + 3)$, and $(N + 5)$. For an island's thickness less than six layers in Fig. 2(a), none of calculated cases agrees with the situations that the value of 3-layer island is larger than that of 2-layer island and the value of the 5-layer island is close to that of the 4-layer island. As comparison is made for island's thickness over six layers [Fig. 2(b)], only the case of $(N + 1)$ fits well with the experimental data, and thus $M = N + 1$. We will discuss that the disagreement in Fig. 2(a) later, which is resulted from the effect of the image potential.

Since the relationship between M and N is determined, the real quantum number of each QW state peak can be assigned, as marked by number near each peak in Figs. 1(c) and 1(d). Figure 2(c) depicts the energy separation of the adjacent peaks for the 13-layer spectrum in Fig. 1(d) (the peak of quantum number 20 is not shown) as a function of the quantum number corresponding to the low-energy one of the adjacent peaks. According to Eq. (1), the energy separation should be linearly proportional to the quantum number, which is displayed with the squares in Fig. 2(c). However, the experimental measurement (circles) significantly deviated from the prediction of Eq. (1); i.e., the energy separation can shrink with increasing the quantum number. This shrinking trend of higher energy QW states is general in all the spectra of Fig. 1. Detail analysis exhibits that the energy separation of quantum number 21 is indeed

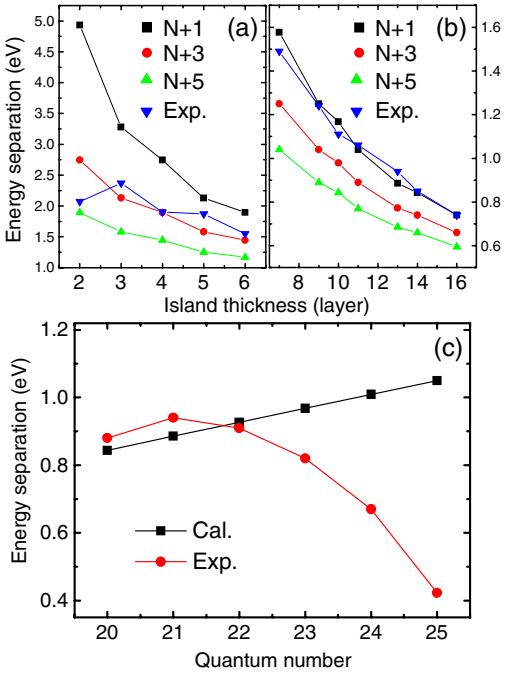

FIG. 2 (color online). Energy separation between the first two peaks in Figs. 1(b) and 1(c) as well as the calculations of $M = (N + 1)$, $(N + 3)$, and $(N + 5)$, as function of island thickness of (a) 2–6 layers and (b) 7–16 layers. (c) Energy separation of adjacent peaks for the calculation and the 13-layer spectrum in Fig. 1(c) as function of the quantum number.

larger than that of quantum number 20, reflecting that the behavior of the QW states near the Fermi level still obeys Eq. (1). The shrinking behavior reminds us of the well-known image-potential states formed near a metal surface [27]. Their energy levels are converged to the vacuum level and also manifest the reduction of level spacing. The analogy of these two phenomena leads us to assume that the energy levels of higher energy QW states could also be influenced by the image potential. In order to prove this assumption, the phase accumulation (PA) model is invoked and a phase ϕ_B is introduced to account for the effect of the image potential [28]. When the potential well in an island is only approximated by the infinite square well, in terms of PA model, there the quantized condition is

$$2k(N + 1)d = 2n\pi. \tag{2}$$

As the image potential is involved, the accumulative phase for quantization becomes

$$2k(N + 1)d + \phi_B = 2n\pi, \tag{3}$$

and

$$\phi_B/\pi = [3.4\ \text{eV}/(E_V - E)]^{1/2} - 1 \tag{4}$$

where E_V is the vacuum level and E is the energy of the QW state and $\hbar^2k^2/2m^* = E + E_F$. Using Eq. (3) and (4), one can calculate E as long as E_V is known.

In principle, the QW state is a bound state, and thus it only exists below the vacuum level. It is hence possible to estimate the vacuum level by observing the highest energy level that the QW state can reach. Figure 3 shows the spectra in the range of 3.5–5 V of the sample bias for Pb islands of varied thickness. It can be seen that the peak location of the highest energy is 4.6 V, as marked by an arrow. We thus assume that E_V for all kinds of thickness is 4.6 eV (dashed lines) and use Eq. (3) and (4) to calculate the energy separation of the adjacent state for the spectrum of the 13-layer island. The calculated energy separations, plotted in Fig. 4(a), display the shrinking character and agree well with the experimental measurements for quantum number above 21. This implies that the higher energy QW states are indeed influenced by the image potential. In addition, with inclusion of the phase contribution of image potential, we also recalculate the energy separation between the first two peaks in Figs. 1(c) and 1(d) for the island's thickness of six layers and less. As exhibited in Fig. 4(b), the calculated values are now consistent with the experimental measurements. This validates the assumed value for E_V in Eq. (4). It has been known that the QW state is inevitably affected by the electric field [26]. However, the phase contributed by the applied bias potential should be different from that by the image potential. Since the experimental data of energy separations can be fit well by introducing the extra phase contribution of the image potential, the influence of the electric field on the energy separation is negligible.

It is evident from Eq. (3) that the shrinking behavior originates from $\phi_B > 0$. Therefore, from Eq. (4), we can determine $E > 1.2$ eV for $\phi_B > 0$ when $E_V = 4.6$ eV. This indicates that the image potential will influence the QW states whose energies are beyond 1.2 eV from the Fermi level. Since the thickness-independent peak in the Fig. 1(d) is located at 0.6 eV, it should not be affected by the image potential. The determination of its quantum number by using $k(N + 1)d = n\pi$ is entirely valid. Further exploiting this peak's wave vector $k = 3\pi/2d$, the bottom of the inner potential in Pb film relative to Fermi

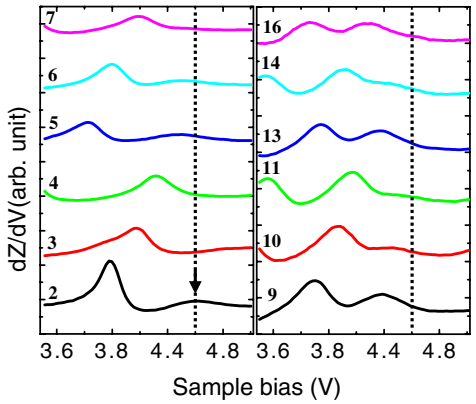

FIG. 3 (color online). Spectra in the range of 3.5–5 V of the sample bias for all kinds of thickness. The arrow marks the highest energy of the peak that we can observe, which is 4.6 eV, and thus the vacuum level is assumed at this energy as well, as indicated by dashed lines.

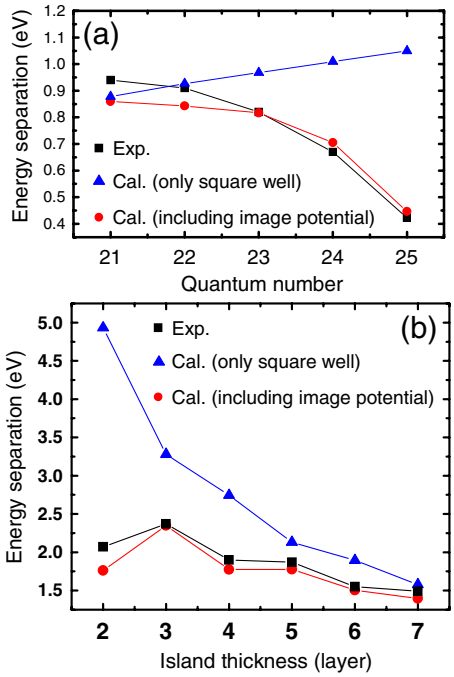

FIG. 4 (color online). The disagreement between the calculations and the experimental results in Figs. 2(a) and 2(c) can be resolved by including the phase contribution of the image potential. (a) and (b) show that the recalculated energy separations can match the experimental results in comparison with the ones of using simple square well.

level can be estimated as $\hbar^2(3\pi/2d)^2/2m^* - 0.6$ eV $=$ 8.48 eV, and thus the depth of the inner potential would be about 8.48 eV + 4.6 eV = 13.08 eV. To our knowledge, this is the first time to quantify the inner potential of a thin film using its QW states.

Since Eq. (2) can describe the QW states for $E <$ 1.2 eV, we infer that the width of the finite square well in the island is Nd. The total effective width should include the depth of electrons penetrating into each side barrier at the Pb/Cu and Pb/vacuum interface, which is roughly $d/2$, and it thus explains $M = N + 1/2 + 1/2 = N + 1$. For $E > 1.2$ eV, we simply add ϕ_B, counting the effect of image potential, to Eq. (2) to form Eq. (3), and with which the higher energy QW states can be described well. This implies that the penetration depth at the Pb/vacuum interface remains existent while the image potential takes part. The image potential is proportional to $1/z$, where z is the perpendicular distance from the metal surface. Electrons always feel the image potential once they are outside the metal. However, the existence of the penetration depth indicates that there exists a quantum regime above the Pb surface where the image potential is vanished. This ingeniously avoids the situation that the image potential becomes infinity when the electron is at the metal surface.

Previous studies by using Z-V spectroscopy to probe the electronic structures of crystal surfaces [29–31] and thin Ag films [32] always exhibited a distinct peak near the vacuum level in the tunneling spectrum. This peak is a quasi-image-potential state formed in the tunneling gap, whose potential form is the superposition of the image potential and the applied bias potential. However, it can be seen that this universal peak disappears in Fig. 3. The creation of this peak, similar to the formation of a standing wave, requires that electrons bounce back and forth in the tunneling gap; i.e., electrons should be reflected from the surface. Once the QW states are formed in the Pb film, electrons can tunnel into the film through these states directly without reflection, causing the disappearance of the quasi-image-potential state. Therefore, this universal state in the vacuum will be quenched if the QW states exist in the films, such as the case of Pb/Cu(111) system shown here.

The authors would like to acknowledge C. S. Kuo, C. Y. Lin, and C. H. Hsieh for their assistance in the construction of low-temperature STM. This work is supported by the National Science Council and Academia Sinica of Taiwan.

[1] D. A. Evans *et al.*, Phys. Rev. Lett. **70**, 3483 (1993).
[2] J. J. Paggel *et al.*, Science **283**, 1709 (1999).
[3] R. K. Kawakami *et al.*, Nature (London) **398**, 132 (1999).
[4] A. Mans *et al.*, Phys. Rev. B **66**, 195410 (2002).
[5] Y. F. Zhang *et al.*, Phys. Rev. Lett. **95**, 096802 (2005).
[6] I. B. Altfeder *et al.*, Phys. Rev. Lett. **78**, 2815 (1997).
[7] I. B. Altfeder *et al.*, Phys. Rev. Lett. **88**, 206801 (2002).
[8] W. B. Su *et al.*, Phys. Rev. Lett. **86**, 5116 (2001).
[9] R. Otero *et al.*, Phys. Rev. B **66**, 115401 (2002).
[10] D. Wegner *et al.*, Phys. Rev. Lett. **94**, 126804 (2005).
[11] S. M. Lu *et al.*, Phys. Rev. B **75**, 113402 (2007).
[12] M. Jałochowski and E. Bauer, Phys. Rev. B **38**, 5272 (1988).
[13] A. Crottini *et al.*, Phys. Rev. Lett. **79**, 1527 (1997).
[14] C. A. Jeffrey *et al.*, Phys. Rev. Lett. **96**, 106105 (2006).
[15] D. A. Luh *et al.*, Science **292**, 1131 (2001).
[16] Y. Guo *et al.*, Science **306**, 1915 (2004).
[17] D. Eom *et al.*, Phys. Rev. Lett. **96**, 027005 (2006).
[18] Y. S. Fu *et al.*, Phys. Rev. Lett. **99**, 256601 (2007).
[19] T. Uchihashi *et al.*, Phys. Rev. B **78**, 033402 (2008).
[20] Y. F. Zhang *et al.*, Appl. Phys. Lett. **90**, 093120 (2007).
[21] E. Ogando *et al.*, Phys. Rev. B **69**, 153410 (2004).
[22] P. M. Echenique and J. B. Pendry, J. Phys. C **11**, 2065 (1978).
[23] T.-C. Chiang, Surf. Sci. Rep. **39**, 181 (2000).
[24] A. M. Shikin *et al.*, Surf. Sci. **487**, 135 (2001).
[25] R. Otero *et al.*, Surf. Sci. **447**, 143 (2000).
[26] S. Ogawa *et al.*, Phys. Rev. B **75**, 115319 (2007).
[27] U. Höfer *et al.*, Science **277**, 1480 (1997).
[28] E. G. McRae, Rev. Mod. Phys. **51**, 541 (1979).
[29] G. Binnig *et al.*, Phys. Rev. Lett. **55**, 991 (1985).
[30] R. S. Becker *et al.*, Phys. Rev. Lett. **55**, 987 (1985).
[31] W. B. Su *et al.*, Phys. Rev. B **75**, 195406 (2007).
[32] W. B. Su *et al.*, J. Phys. Condens. Matter **18**, 6299 (2006).